

J. N. Low,^a M. D. López,^a P. Arranz Mascarós,^b J. Cobo Domingo,^b M. L. Godino,^b R. López Garzón,^b M. D. Gutiérrez,^b M. Melguizo,^b G. Ferguson^c and C. Glidewell^{d*}

^aDepartment of Applied Physics and Electronic and Mechanical Engineering, University of Dundee, Dundee DD1 4HN, Scotland,

^bDepartamento de Química Inorgánica y Orgánica, Universidad de Jaén, 23071 Jaén, Spain,

^cDepartment of Chemistry and Biochemistry, University of Guelph, Guelph, Ontario, Canada N1G 2W1, and ^dSchool of Chemistry, University of St Andrews, St Andrews KY16 9ST, Scotland

Correspondence e-mail: cg@st-andrews.ac.uk

N-(6-Amino-3,4-dihydro-3-methyl-5-nitroso-4-oxopyrimidin-2-yl) derivatives of glycine, valine, serine, threonine and methionine: interplay of molecular, molecular–electronic and supramolecular structures

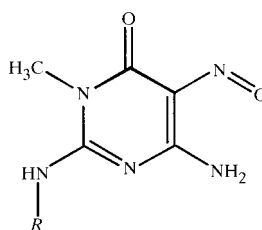
Received 23 March 2000

Accepted 7 April 2000

In each of *N*-(6-amino-3,4-dihydro-3-methyl-5-nitroso-4-oxopyrimidin-2-yl)valine, C₁₀H₁₅N₅O₄ (3) (orthorhombic, *P*2₁2₁2₁), *N*-(6-amino-3,4-dihydro-3-methyl-5-nitroso-4-oxopyrimidin-2-yl)serine monohydrate, C₈H₁₁N₅O₅·H₂O (4) (orthorhombic, *P*2₁2₁2₁), and *N*-(6-amino-3,4-dihydro-3-methyl-5-nitroso-4-oxopyrimidin-2-yl)threonine, C₉H₁₃N₅O₅ (5) (monoclinic, *P*2₁), the C–nitroso fragments exhibit almost equal C–N and N–O bond lengths: the C–N range is 1.315 (3)–1.329 (3) Å and the N–O range is 1.293 (3)–1.326 (3) Å. In each compound there are also very short intermolecular O–H···O hydrogen bonds, in which carboxyl groups act as hydrogen-bond donors to the nitrosyl O atoms: the O···O distances range from 2.440 (2) to 2.504 (4) Å and the O–H···O angles lie between 161 and 163°. An interpretation of the relationship between the unusual intramolecular bond lengths and the very short intermolecular hydrogen bonds has been developed based on database analysis and computational modelling. In each of (3)–(5) there is an extensive network of intermolecular hydrogen bonds, generating three-dimensional frameworks in (3) and (5), and two-dimensional sheets in (4).

1. Introduction

The crystal structures of (1) (Low *et al.*, 1997) and (2) (Low *et al.*, 1999) are both characterized by very short intermolecular O–H···O hydrogen bonds involving the carboxylic acid function as the hydrogen-bond donor and the nitrosyl O atom



- (1) *R* = CH₂COOH·2H₂O
 (2) *R* = CH(COOH)CH₂CH₂SCH₃
 (3) *R* = CH(COOH)CH(CH₃)₂
 (4) *R* = CH(COOH)CH₂OH·H₂O
 (5) *R* = CH(COOH)CH(OH)CH₃
 (6) *R* = H

as the acceptor: in these hydrogen bonds, the O···O distances, 2.491 (3) and 2.473 (2) Å, respectively, are typical of those found in ionic O–H···O[−] hydrogen bonds. Here we report the structures of the related compounds (3)–(5), which all exhibit this same feature, and we interpret this by reference to a systematic study of geometric data for related systems

retrieved from the Cambridge Structural Database (CSD; Allen & Kennard, 1993) and by the use of computational modelling of the molecular and electronic structure of the reference compound (6)

2. Experimental

2.1. Synthesis

Samples of (3)–(5) were prepared by the addition of a suspension of 6-amino-3,4-dihydro-3-methyl-2-methoxy-5-nitroso-4-oxypyrimidine in acetonitrile (3 cm^3 per mmol of the pyrimidine) to a suspension of the corresponding L-amino acid (1.1 molar equiv.) in aqueous KOH solution (0.5 mol dm^{-3} ; 2 cm^3 per mmol of amino acid). In each case the mixture was stirred at 343 K for 1 h, after which it was cooled to ambient temperature, acidified to pH = 3 and reduced to half volume. The resulting crystalline solids were filtered off and washed successively with water, ethanol and diethyl ether. *N*-(6-Amino-3,4-dihydro-3-methyl-5-nitroso-4-oxypyrimidin-2-yl)-valine (3), m.p. 524 K (dec.), analysis: found C 44.6, H 5.6, N 26.0%; $\text{C}_{10}\text{H}_{15}\text{N}_5\text{O}_4$ requires C 44.3, H 5.6, N 25.8%. *N*-(6-Amino-3,4-dihydro-3-methyl-5-nitroso-4-oxypyrimidin-2-yl)-serine monohydrate (4), m.p. 450 K (dec.), analysis: found C 34.8, H 4.4, N 24.7%; $\text{C}_8\text{H}_{13}\text{N}_5\text{O}_6$ requires C 34.9, H 4.7, N 25.5%. *N*-(6-Amino-3,4-dihydro-3-methyl-5-nitroso-4-oxypyrimidin-2-yl)threonine (5), m.p. 484 K (dec.), analysis: found C 39.7, H 4.9, N 25.7%; $\text{C}_9\text{H}_{13}\text{N}_5\text{O}_5$ requires C 39.9, H 4.8, N 25.8%. Crystals suitable for single-crystal X-ray diffraction were selected directly from the analytical samples.

2.2. Data collection, structure solution and refinement

Details of cell data, data collection and refinement are summarized in Table 1 (Enraf–Nonius, 1992; Gabe *et al.*, 1989; Ferguson, 1998, 1999; Nonius, 1997; Otwinowski & Minor, 1997; Sheldrick, 1997*a,b*; Spek, 1999). For (3) and (4) the space group $P2_12_12_1$ was uniquely determined from the systematic absences. For (5) the systematic absences permitted the space groups $P2_1$ and $P2_1/m$; in view of the chiral nature of the amino-acid fragment, the space group $P2_1$ was chosen and confirmed by the subsequent structure solution and refinement. The structures were all solved by direct methods using *SHELXS97* (Sheldrick, 1997*b*) and refined on F^2 with all data using *SHELXL97* (Sheldrick, 1997*a*). A weighting scheme based upon $P = [F_o^2 + 2F_c^2]/3$ was employed in order to reduce statistical bias (Wilson, 1976). All H atoms were located from difference maps and all were included in the refinements as riding atoms.

In (3) the orientation of the isopropyl group was modelled by the use of two sets of sites, whose site-occupation factors refined to 0.701 (6) and 0.299 (6), respectively: the two methyl C atoms in the minor component were refined isotropically. In addition, the H atoms of the methyl groups in (3) were all modelled by two sets of sites offset by a 60° rotation about the terminal C–C bonds and each with 0.50 occupancy relative to the associated C atom. In none of (3)–(5) is there any atom heavier than O; hence, the Friedel equivalents were all merged

before refinement. In each case the overall chirality was selected using the known chirality of the amino-acid starting materials: the configuration at C21 is always *S*, as required by L-amino acids, and that at C22 in (5) is *R*.

The diagrams were prepared with the aid of *PLATON* (Spek, 1999). Figs. 1–3 show the molecular structures of (3)–(5), Fig. 4 shows the correlations between N–O, C–N and O···O distances, and Figs. 5–12 show aspects of the crystal structures; in some of the packing diagrams, the atom-labelling has been placed on a molecule outside the unit cell, for the sake of clarity. Selected molecular dimensions are presented in Tables 2 and 3; C-nitroso compounds retrieved from the CSD are identified in Table 4; C details of the hydrogen bonding are given in Table 5.

2.3. Molecular modelling

Computations of molecular geometry and energy were made using the *AM1* method (Dewar *et al.*, 1985), as implemented in *MOPAC*, version 6 (Stewart, 1990). Each stationary point was characterized by calculation of the force-constant matrix. The polarization entity employed was simulated by an integer charge at the centre of a repulsion sphere of the form $\exp(-\alpha r)$, in effect a unit charge delocalized over the surface of a hard sphere of diameter 1.4 Å (Stewart, 1990). Selected conformational data are given in Table 2.¹

3. Results and discussion

3.1. Molecular structures of (3)–(5)

The molecular conformations of (1)–(5) are all very similar, despite the differences between the side chains in terms both of their steric demands and of their hydrogen-bonding capacity. The pyrimidinone rings are all essentially planar, and both the amino and the nitrosyl substituents are coplanar with the ring (Table 2): only the *N*-substituent side chains deviate from this plane and, except for (1), where there is no carbon substitution at C21, the dispositions even of these chains are very similar, as illustrated by the torsion angles C2–N2–C21–C22 and C2–N2–C21–C211 (Table 2). The coplanarity of the amino groups with the pyrimidinone ring permits electronic delocalization between the various N atoms, but effectively precludes these atoms from acting as hydrogen-bond acceptors. In each compound the nitrosyl group is oriented *trans* to C4, so that its oxygen O5 is ideally placed for the formation of an intramolecular N–H···O hydrogen bond in an *S*(6) motif (Bernstein *et al.*, 1995).

Several of the bond lengths in (1)–(5) have unexpected values. First, in the C-nitroso group the C–N and N–O bond distances are almost identical (Table 3): in simple neutral compounds where there is no possibility of significant electronic delocalization these distances normally differ by at least 0.20 Å (Talberg, 1977; Schlemper *et al.*, 1986) and the NO distance rarely exceeds 1.25 Å (Davis *et al.*, 1965; Bauer &

¹Supplementary data for this paper are available from the IUCr electronic archives (Reference: NA0105). Services for accessing these data are described at the back of the journal.

Table 1

Experimental details.

	(3)	(4)	(5)
Crystal data			
Chemical formula	C ₁₀ H ₁₅ N ₅ O ₄	C ₈ H ₁₁ N ₅ O ₅ ·H ₂ O	C ₉ H ₁₃ N ₅ O ₅
Chemical formula weight	269.27	275.23	271.24
Cell setting	Orthorhombic	Orthorhombic	Monoclinic
Space group	<i>P</i> 2 ₁ 2 ₁ 2 ₁	<i>P</i> 2 ₁ 2 ₁ 2 ₁	<i>P</i> 2 ₁
<i>a</i> (Å)	8.9136 (6)	6.5574 (7)	8.3686 (3)
<i>b</i> (Å)	11.2501 (6)	7.686 (2)	6.7077 (3)
<i>c</i> (Å)	13.0585 (12)	22.222 (3)	11.1230 (4)
β (°)	90	90	111.265 (2)
<i>V</i> (Å ³)	1309.49 (16)	1119.9 (4)	581.86 (4)
<i>Z</i>	4	4	2
<i>D_x</i> (Mg m ⁻³)	1.366	1.632	1.548
Radiation type	Mo <i>K</i> α	Mo <i>K</i> α	Mo <i>K</i> α
Wavelength (Å)	0.7093	0.7107	0.71073
No. of reflections for cell parameters	25	25	1434
θ range (°)	9.31–18.93	10.0–12.50	1.96–27.41
μ (mm ⁻¹)	0.108	0.140	0.128
Temperature (K)	294 (1)	294 (1)	150.0 (1)
Crystal form	Needle	Block	Block
Crystal size (mm)	0.42 × 0.29 × 0.28	0.24 × 0.18 × 0.12	0.20 × 0.20 × 0.20
Crystal colour	Orange	Orange	Orange
Data collection			
Diffractometer	CAD-4	CAD-4	Kappa-CCD
Data collection method	$\theta/2\theta$ scans	$\theta/2\theta$ scans	φ scans and ω scans with κ offsets
Absorption correction	None	None	Multi-scan
<i>T</i> _{min}	–	–	0.941
<i>T</i> _{max}	–	–	0.975
No. of measured reflections	3011	2082	5604
No. of independent reflections	1738	1239	1434
No. of observed reflections	1375	791	1271
Criterion for observed reflections	<i>I</i> > 2σ(<i>I</i>)	<i>I</i> > 2σ(<i>I</i>)	<i>I</i> > 2σ(<i>I</i>)
<i>R</i> _{int}	0.019	0.062	0.036
θ_{\max} (°)	27.42	25.41	27.41
Range of <i>h, k, l</i>	–11 → <i>h</i> → 11 –14 → <i>k</i> → 14 –16 → <i>l</i> → 16	–7 → <i>h</i> → 7 –9 → <i>k</i> → 9 –26 → <i>l</i> → 26	–10 → <i>h</i> → 10 –7 → <i>k</i> → 8 –12 → <i>l</i> → 14
No. of standard reflections	3	3	0
Frequency of standard reflections	Every 120 min	Every 180 min	–
Intensity decay (%)	0.7	0	0
Refinement			
Refinement on	<i>F</i> ²	<i>F</i> ²	<i>F</i> ²
<i>R</i> [<i>F</i> ² > 2σ(<i>F</i> ²)]	0.0440	0.0520	0.0367
<i>wR</i> (<i>F</i> ²)	0.1260	0.1113	0.0946
<i>S</i>	1.036	0.977	1.029
No. of reflections used in refinement	1738	1239	1434
No. of parameters used	185	176	177
H-atom treatment	H-atom parameters constrained	H-atom parameters constrained	H-atom parameters constrained
Weighting scheme	$w = 1/[\sigma^2(F_o^2) + (0.0782P)^2 + 0.2134P]$, where $P = (F_o^2 + 2F_c^2)/3$	$w = 1/[\sigma^2(F_o^2) + (0.0524P)^2]$, where $P = (F_o^2 + 2F_c^2)/3$	$w = 1/[\sigma^2(F_o^2) + (0.0537P)^2 + 0.1096P]$, where $P = (F_o^2 + 2F_c^2)/3$
(Δ/σ) _{max}	0.000	0.004	0.002
$\Delta\rho_{\max}$ (e Å ⁻³)	0.277	0.200	0.335
$\Delta\rho_{\min}$ (e Å ⁻³)	–0.252	–0.201	–0.387
Extinction method	None	None	SHELXL97 (Sheldrick, 1997b)
Extinction coefficient	–	–	0.028 (7)
Source of atomic scattering factors	<i>International Tables for Crystallography</i> (1992, Vol. C, Tables 4.2.6.8 and 6.1.1.4)	<i>International Tables for Crystallography</i> (1992, Vol. C, Tables 4.2.6.8 and 6.1.1.4)	<i>International Tables for Crystallography</i> (1992, Vol. C, Tables 4.2.6.8 and 6.1.1.4)
Computer programs			
Data collection	CAD-4 (Enraf–Nonius, 1992)	CAD-4 (Enraf–Nonius, 1992)	Kappa-CCD (Nonius, 1997)
Cell refinement	SET4 and CELDIM (Enraf–Nonius, 1992)	SET4 and CELDIM (Enraf–Nonius, 1992)	DENZO (Otwinowski & Minor, 1997)
Data reduction	DATRD2 in NRCVAX96 (Gabe <i>et al.</i> , 1989)	DATRD2 in NRCVAX96 (Gabe <i>et al.</i> , 1989)	DENZO (Otwinowski & Minor, 1997)
Structure solution	SHELXS97 (Sheldrick, 1997a)	SHELXS97 (Sheldrick, 1997a)	SHELXS97 (Sheldrick, 1997a)
Structure refinement	SHELXL97 (Sheldrick, 1997b)	SHELXL97 (Sheldrick, 1997b)	SHELXL97 (Sheldrick, 1997b)
Preparation of material for publication	SHELXL97 and WordPerfect macro PREP8 (Ferguson, 1998)	SHELXL97 and WordPerfect macro PREP8 (Ferguson, 1998)	SHELXL97 and WordPerfect macro PRPKAPPA (Ferguson, 1999)

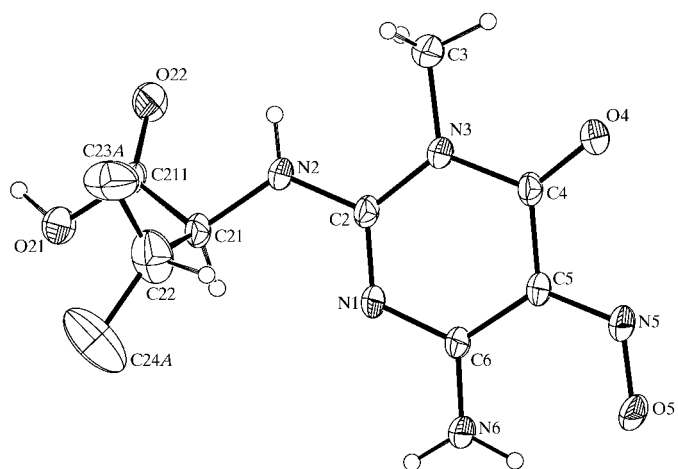
Table 2

Selected torsional angles for (1)–(5) (°).

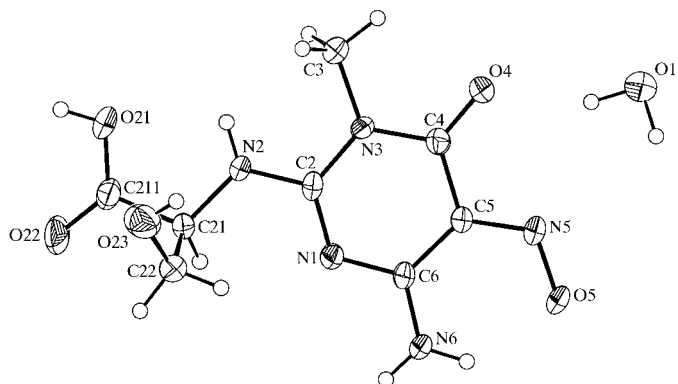
 For (1) see Low *et al.* (1997) and for (2) see Low *et al.* (1999) [original atom-labelling altered to be consistent with that in (3)–(5)].

	(1)	(2)	(3)	(4)	(5)
$\delta(\text{O5}-\text{N5}-\text{C5}-\text{C4})$	-178.8 (2)	-177.2 (2)	-177.7 (2)	179.2 (5)	177.4 (2)
$\delta(\text{N1}-\text{C2}-\text{N2}-\text{C21})$	-0.7 (3)	-4.7 (4)	1.4 (4)	2.5 (8)	5.4 (3)
$\delta(\text{C2}-\text{N2}-\text{C21}-\text{C22})$	-	83.5 (3)	94.5 (3)	74.5 (6)	104.3 (2)
$\delta(\text{C2}-\text{N2}-\text{C21}-\text{C211})$	-81.3 (3)	-151.0 (2)	-140.1 (3)	-165.6 (4)	-131.9 (2)
$\delta(\text{C2}-\text{N2}-\text{C21}-\text{C22})_{\text{calc.}}$	-	69.9	69.1	64.5	68.8
$\delta(\text{C2}-\text{N2}-\text{C21}-\text{C211})_{\text{calc.}}$	-79.3	-169.2	-168.9	-174.8	-167.9

Andreassen, 1972; Talberg, 1977; Schlemper *et al.*, 1986). On the other hand, the C–N and N–O distances in (1)–(5) are entirely typical of those observed in oximate anions [$\text{RR}'\text{C}=\text{N}-\text{O}^-$] [(11)–(14) and (18), Table 4; Raston *et al.*, 1978; Domasevitch, Gerasimchuk *et al.*, 1996, Domasevitch, Mokhir & Rusanov, 1996; Domasevitch *et al.*, 1997, 1998]. Associated with the unusual C–N–O geometry in each of (1)–(5) is a very short hydrogen bond between the carboxylic

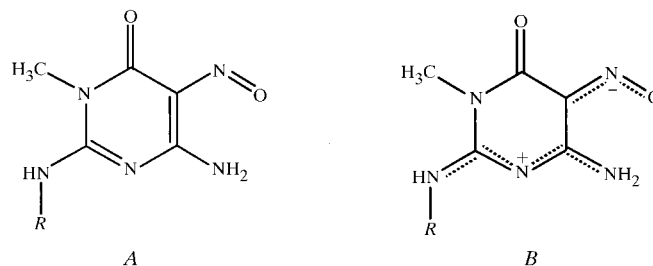

Figure 1

The asymmetric unit of (3), showing the atom-labelling scheme. Displacement ellipsoids are drawn at the 30% probability level. For the sake of clarity only the major orientation of the disordered side chain is shown.

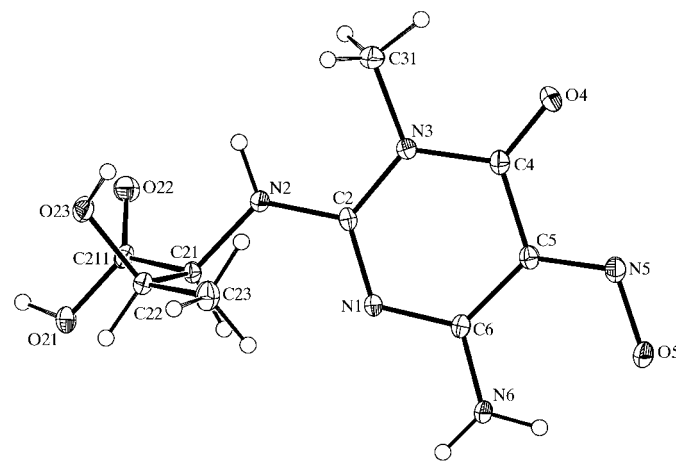

Figure 2

The asymmetric unit of (4), showing the atom-labelling scheme. Displacement ellipsoids are drawn at the 30% probability level.

acid function in one molecule and the nitrosyl O in another, having O...O distances in the range 2.440 (2) Å in (5) to 2.504 (4) Å in (4) (see also §3.3). These distances are typical of those in ionic hydrogen bonds of O–H...O– type, but the unambiguous location, from difference maps, of the carboxylic H atoms as well as the clear difference between the two independent C–O distances indicate that in none of (1)–(5) has there been any proton transfer from the carboxylic acid group. Secondly, the C5–C6 bond length in each of (1)–(5) is more typical of a single bond between two three-connected C atoms [mean value 1.460 Å (Allen *et al.*, 1987)] than of a double bond between two such atoms [mean value for C-substituted bonds 1.331 Å; typical values in N heterocycles lie in the range 1.36–1.38 Å (Allen *et al.*, 1987)]. Thirdly, the N1–C2 bond, although shorter than the C2–N2 and N1–C6 bonds in (2), (4) and (5), is consistently longer than the C6–N6 bond: in (3), the length of the N1–C2 bond is not significantly different from those of the C2–N2 and N1–C6 bonds. In all cases the N1–C2 bond length is between



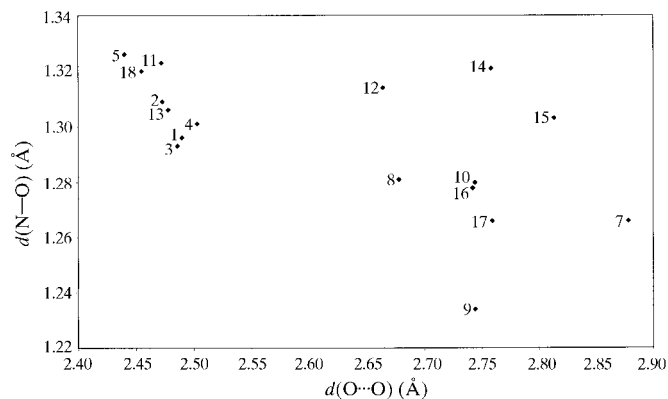
the mean values found for $\text{Csp}^2-\text{N}(2)$ and $\text{Csp}^2=\text{N}(2)$ bond lengths, 1.376 and 1.279 Å, respectively, but is rather similar to the mean C–N bond length, 1.328 Å, found in substituted guanidinium cations (Allen *et al.*, 1987). These geometric parameters taken together indicate that the conventional


Figure 3

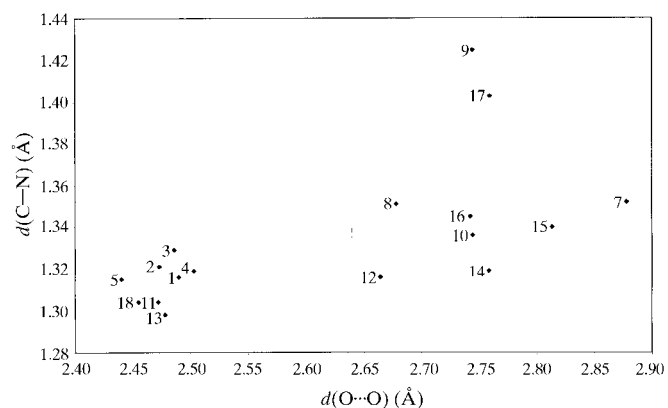
The asymmetric unit of (5), showing the atom-labelling scheme. Displacement ellipsoids are drawn at the 30% probability level.

representation *A* is a less appropriate representation of the molecular and electronic structure in this series than the alternative, charge-separated form *B*

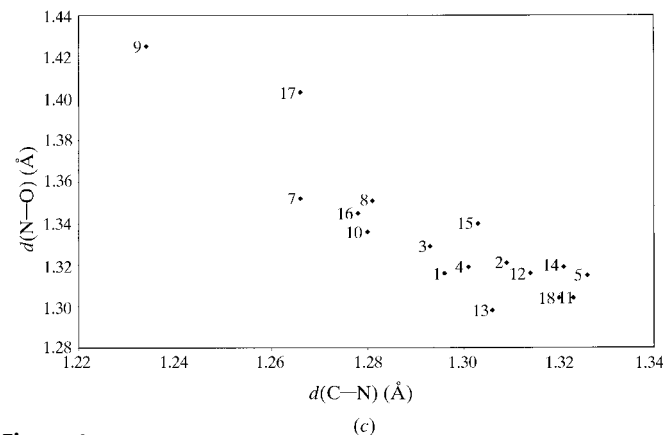
Form *B* not only accommodates the long C5–C6 bond and the similar C–N distances involving N1, N2 and N6, but most significantly it accommodates the near similarity of the C5–N5 and N5–O5 distances in the C–N–O fragments and at the same time indicates the development of significant negative charge at O5, essential for the formation of very short intermolecular O–H···O hydrogen bonds. While form *A* is



(a)



(b)



(c)

Figure 4

Plots of N–O, C–O and O···O distances in (1)–(5) and in related C-nitroso compounds retrieved from the CSD (Allen & Kennard, 1993): (a) N–O and O···O distances; (b) C–N and O···O distances; (c) N–O and C–N distances. Compounds (7)–(18) are identified in Table 4.

the better representation for many examples, it is clear that in the solid state it is possible to perturb the electronic structure towards form *B*. The conditions under which such perturbation occurs are explored in the following sections which describe database studies and computer modelling.

3.2. Comparisons with related compounds

The observation in (1)–(5) of consistently unusual intramolecular geometry, as judged against the generalized data in Allen *et al.* (1987), prompted us to undertake a more systematic study using more specific data retrieved from the CSD (Allen & Kennard, 1993). First, all structures were retrieved which contained a CNO fragment in which the C atom was bonded to two, and only two, other C atoms; in which the N atom was exactly two-coordinate; and in which the O atom could either be bonded solely to N or to N and H: the search criteria also specified $R < 0.10$ and no disorder. For all the structure thus retrieved, (7)–(18) (identified in Table 4), and with compounds (1)–(5) added in to the data pool, plots of both the CN and NO distances in the CNO fragment against the shortest non-bonded O···O distances involving the CNO fragment revealed two distinct domains (Fig. 4). In one domain the maximum O···O distance was 2.504 (4) Å, in (4), while in the other the minimum O···O distance was

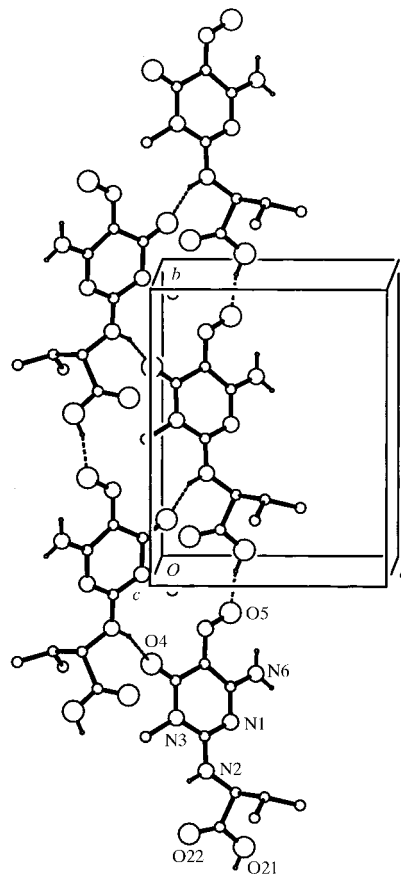
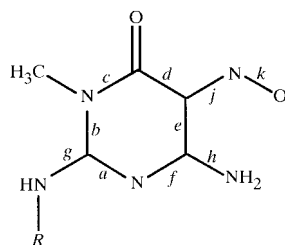


Figure 5

Part of the crystal structure of (3), showing the formation of a C(11) chain by translation and a C(6) spiral, both parallel to [010]. H atoms bonded to C are omitted for the sake of clarity.

Table 3
Selected interatomic distances for (1)–(6) (Å).



<i>R</i>	<i>a</i>	<i>b</i>	<i>c</i>	<i>d</i>	<i>e</i>	<i>f</i>	<i>g</i>	<i>h</i>	<i>j</i>	<i>k</i>
CH ₂ COOH	1.323 (3)	1.376 (3)	1.381 (3)	1.469 (3)	1.444 (3)	1.332 (3)	1.319 (3)	1.331 (3)	1.316 (3)	1.296 (2)
CH ₂ (COOH)CH ₂ CH ₂ SMe	1.313 (4)	1.384 (3)	1.401 (3)	1.467 (4)	1.456 (4)	1.334 (3)	1.335 (3)	1.308 (4)	1.321 (3)	1.309 (3)
CH(COOH)CHMe ₂	1.313 (3)	1.374 (3)	1.404 (3)	1.453 (4)	1.450 (3)	1.345 (3)	1.337 (3)	1.303 (4)	1.329 (3)	1.293 (3)
CH(COOH)CH ₂ OH	1.311 (6)	1.385 (5)	1.379 (5)	1.461 (6)	1.451 (6)	1.334 (5)	1.331 (5)	1.303 (5)	1.319 (5)	1.301 (5)
CH(COOH)CH(OH)Me	1.337 (3)	1.374 (3)	1.400 (3)	1.479 (3)	1.458 (3)	1.333 (3)	1.333 (3)	1.311 (3)	1.315 (3)	1.326 (3)
H [†]	1.357	1.402	1.437	1.464	1.436	1.389	1.396	1.363	1.416	1.170
H [‡]	1.383	1.403	1.425	1.510	1.501	1.354	1.364	1.349	1.317	1.285
H [§]	1.377	1.401	1.429	1.490	1.475	1.362	1.371	1.355	1.350	1.221

[†] Calculated for isolated neutral molecules. [‡] Calculated with H⁺ on nitrosyl O. [§] Calculated with +1 polarization charge 1.55 Å from nitrosyl O.

2.664 (5) Å (ROLNEL; Domasevitch *et al.*, 1996*b*). Moreover, those examples in the short O···O domain all had absolute values of $\Delta = |d(\text{C}-\text{N}) - d(\text{N}-\text{O})|$ no greater than 0.020 Å: on the other hand, neutral compounds in the long O···O domain all had $\Delta > 0.060$ Å and only two, ROLNEL and SEOBOX (Raston *et al.*, 1978), had $\Delta < 0.020$ Å. It is striking that these two compounds are both salts, but that neither of them contains any donors suitable for the formation of strong O–H···O hydrogen bonds, thus precluding the occurrence of

short O···O distances. The near-identity of the C–N and N–O distances in CNO fragments thus appears to be associated with either extremely short O–H···O hydrogen bonds in which the nitrosyl O is the acceptor, or, in their absence, with ionic systems containing no strong hydrogen-bond donors. The near-complementary nature of the plots in Figs. 4(*a*) and (*b*) implies a strong correlation between the N–O and C–N distances, Fig. 4(*c*): as expected from the possible canonical structures for a fragment $[\text{RR}'\text{C}=\text{N}-\text{O}]^-$, a long N–O bond is associated with a short C–N bond, and *vice versa*.

A second search was then undertaken to retrieve all neutral compounds containing the 2,6-diaminopyrimidine fragment,

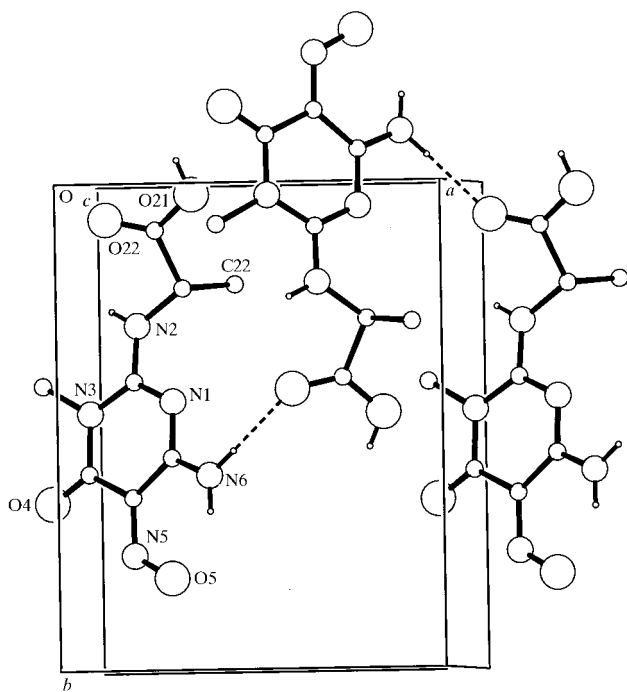


Figure 6
Part of the crystal structure of (3), showing the formation of a C(9) spiral, running parallel to [100]. Atoms are depicted as in Fig. 5, but for the sake of clarity the disordered atoms of the side chain are omitted.

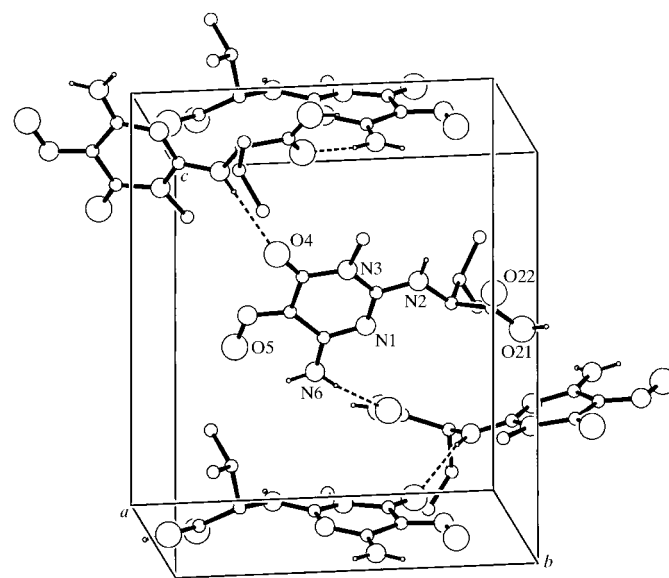
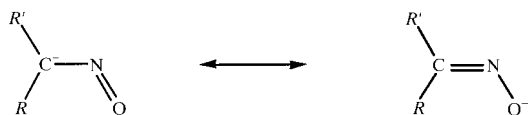


Figure 7
Part of the crystal structure of (3), showing a C₂²(11) spiral parallel to [001]. Atoms are depicted as in Fig. 5.

Table 4
C–Nitroso compounds related to (1)–(5), retrieved from the CSD.

Number	CSD code	Reference
(7)	HEKXOK	Low <i>et al.</i> (1994)
(8)	NHQUSA	Korvenranta <i>et al.</i> (1978)
(9)	NTSALA	Talberg (1977)
(10)	NUSDUA	Schwabenlander <i>et al.</i> (1998)
(11)	PAOPEC	Domasevitch <i>et al.</i> (1998)
(12)	ROLNEL	Domasevitch <i>et al.</i> (1996b)
(13)	ROMXAS	Domasevitch <i>et al.</i> (1997)
(14)	SEOBOS	Raston <i>et al.</i> (1978)
(15)	SNTOSP	Talberg (1975)
(16)	SORTAU	Pecorari <i>et al.</i> (1991)
(17)	SRVIOL	Hamelin (1976)
(18)	TUHSIY	Domasevitch <i>et al.</i> (1996a)

again subject to the criteria of $R < 0.10$ and no disorder, in order to compare the C–N and C–C bond lengths with those



in (1)–(5): *N*-protonated systems and *N*-oxides were excluded from this selection. Although the ranges spanned by individual bonds in the nitrosyl-free examples retrieved from the CSD are typically between 0.020 and 0.040 Å, for several of the

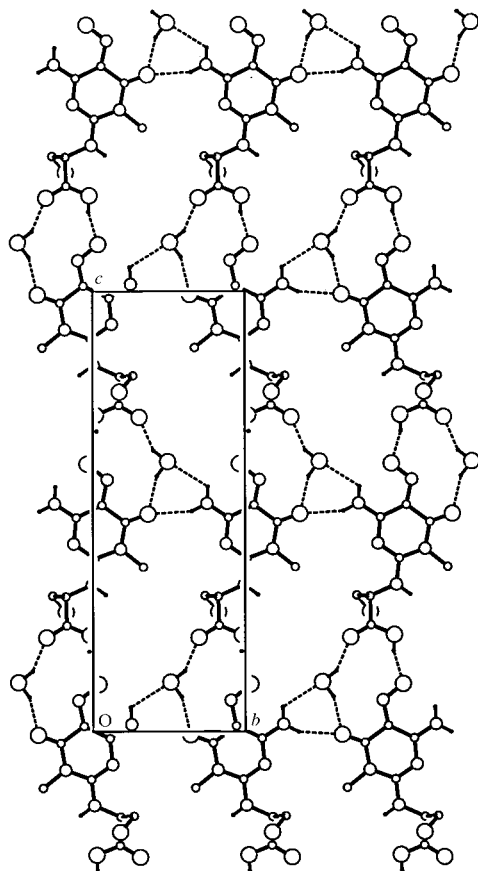
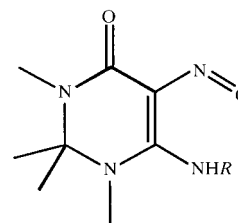


Figure 8
Part of the crystal structure of (4), showing the formation of a (100) sheet. Atoms are depicted as in Fig. 5.

individual bonds there is no overlap at all of the ranges spanned by nitrosyl-free systems on the one hand and (1)–(5) on the other. For example, the C5–C6 bond, where the observed distances in (1)–(5) range from 1.444 (3) Å in (1) to 1.458 (3) Å in (5), is always much shorter in the absence of a nitrosyl group where the longest recorded value is 1.424 (5) Å (DUZHAI; Maag *et al.*, 1986), and there is similarly no overlap of ranges for the C2–N3 bond, where the largest retrieved value is 1.358 (5) Å (VUJGOW; Griffin & Lowe, 1992). For the exocyclic C–N bonds, there is no overlap of ranges for C6–N6, where the shortest value retrieved is 1.321 (2) Å (KEGPUH; Lehn *et al.*, 1990); however, the ranges just overlap for the C2–N2 bond, where the retrieved values range from 1.408 (5) Å (VUJGOW) to 1.333 (5) Å (BIGCUP; Shimizu *et al.*, 1982). These findings amply confirm the deductions made above (see §3.1) that the exocyclic C–N bonds in (1)–(5) are all unusually short for single bonds of their type, while the C5–C6 bonds are unusually long for C=C double bonds.

Finally, a third search was conducted, using the same acceptance criteria as before, to retrieve all neutral compounds containing the fragment



but in which there are no strong hydrogen-bond donor groups. The purpose of this selection was to assess the effect of the

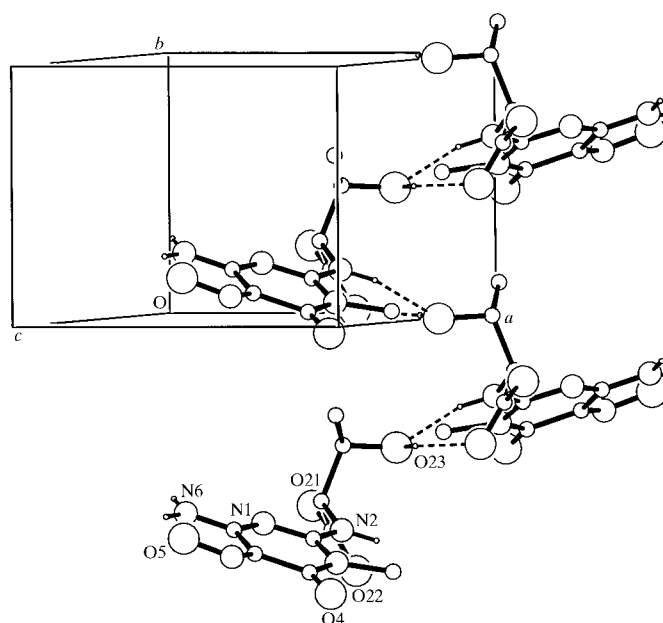
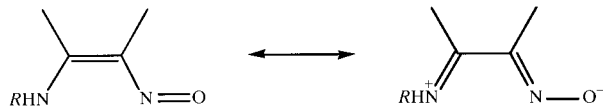


Figure 9
Part of the crystal structure of (5), showing the formation of a spiral parallel to [010] around $(1, y, \frac{1}{2})$. Atoms are depicted as in Fig. 5.

adjacent amino function on the dimensions of the nitrosyl group, *i.e.* the extent of the delocalization.

In every example, the value of Δ was typical of those found earlier in the long O...O domain, ranging from 0.067 Å (SORTAU; Pecorari *et al.*, 1991) to 0.086 Å (HEKXOK; Low *et al.*, 1994). Hence, while the adjacent amino group effects



some reduction in the magnitude of Δ from the values of *ca* 0.20 Å or more found in very simple C-nitroso compounds, nonetheless, its effect is clearly insufficient to account for the very low value of Δ found in (1)–(5).

3.3. Modelling the molecular and electronic structures

3.3.1. Molecular conformations. For isolated molecules of (1)–(5) two conformational minima were found in the rotation of the substituent around the bond N2–C21. For (1) the two conformers were mirror images, with identical ΔH_f^0 values at the minima and calculated torsional angles C2–N2–C21–C211 of $\pm 79.3^\circ$, remarkably close to the observed values of $-81.3(3)^\circ$ (Low *et al.*, 1997). For each of (2)–(5) again two conformational minima were found, but with marginally different torsional angles and ΔH_f^0 values, because of the stereogenic centre at C21 which precludes the conformers from being mirror images. In every case, however, the calculated energy difference between the global conformational minimum and the top of the rotational energy barrier was

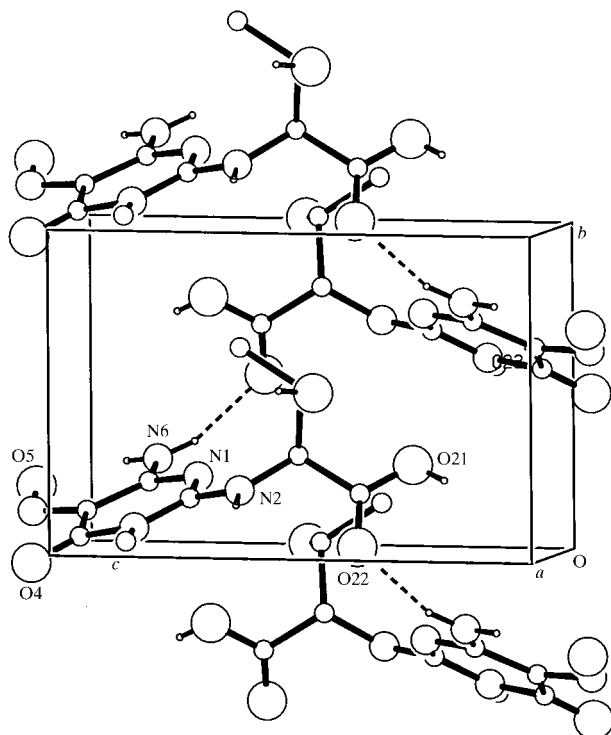


Figure 10
Part of the crystal structure of (5), showing the formation of a spiral parallel to [010] around $(\frac{1}{2}, y, \frac{1}{2})$. Atoms are depicted as in Fig. 5.

25 kJ mol⁻¹ or less, so that in all compounds modest perturbations from the conformational minima can readily be achieved through the agency of the intermolecular forces, particularly the hydrogen bonds involving the carboxyl groups.

The calculated values of the key torsional angles involving the side chains are included in Table 1, along with the observed values. The maximum difference between observed and calculated torsional angles occurs for (5), but even with a difference here of almost 40° the calculated energy cost of this perturbation is only *ca* 3.25 kJ mol⁻¹. Hence, the observed conformations all represent perturbations from the conformational minima associated with very low energy costs, readily recouped from the energies of the strong hydrogen bonds. The close agreement between the observed and calculated conformations in (1) is undoubtedly fortuitous.

3.3.2. Molecular and electronic structures. Regardless of the side-chain conformations, the bond lengths and angles for the substituted pyrimidinone portion calculated for isolated molecules were remarkably similar for all (1)–(5) and also for the reference compound (6), where R = H. Hence, for simplicity of calculation and comparison, all subsequent calculations were carried out on (6).

For isolated molecules of (6), the calculated values of the C–N and N–O bond lengths in the C-nitrosyl fragment are 1.416 and 1.170 Å, so that Δ (see §3.2) is 0.246 Å: the corresponding bond orders calculated for C–N and N–O are 1.090 and 1.811, respectively. Hence, these results indicate essentially no electronic delocalization into the C–N–O fragment. Of the other C–N and C–C bonds, C1–N2 had by far the highest bond order, 1.406, but the bond orders for C2–N2, N1–C6 and C6–N6 were all above unity, while those for C4–O4 and C5–C6 were 1.797 and 1.221, respectively; these results indicate some modest delocalization from the N atoms to the amidic oxygen, but an isolated nitrosyl group. However, the molecular and electronic structure is drastically perturbed by the introduction of positive polarization in the vicinity of the nitrosyl group.

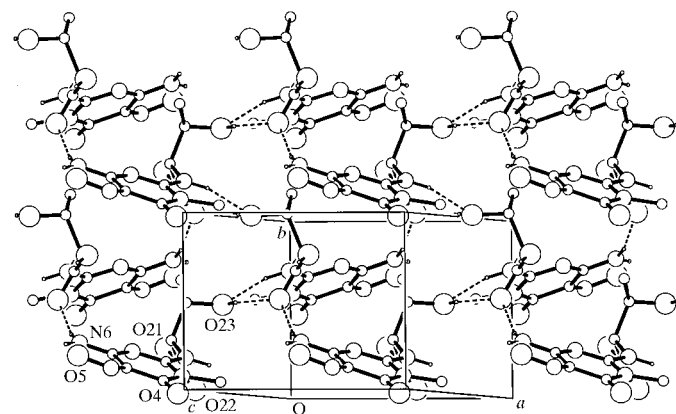
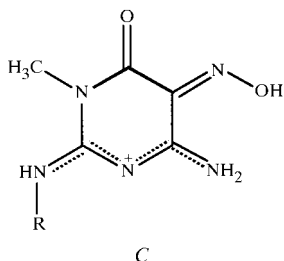


Figure 11
Part of the crystal structure of (5), showing [010] spirals around $(0, y, \frac{1}{2})$, $(\frac{1}{2}, y, \frac{1}{2})$ and $(1, y, \frac{1}{2})$ giving rise to an (001) sheet. Atoms are depicted as in Fig. 5.

Protonation of O5 (Figs. 1–3) leads to a calculated value of Δ of 0.032 Å, close to the values observed in (1)–(5), and a molecular and electronic structure well described by the single canonical form *C*, including a very long C5–C6 bond and close similarity of the C–N bond lengths involving N1, N2 and N6.



When a more realistic source of polarization was employed, namely a diffuse unit charge, placed *ca* 1.55 Å from O5 (*cf.* the observed hydrogen-bond O···H distances, Table 5), this generated C5–N5 and N5–O5 bond orders of 1.480 and 1.394, respectively, a long C5–C6 bond and extensive delocalization in the bonds N2–C2, C2–N1, N1–C6 and C6–N6. In effect, the canonical form *B* (see §3.1) is almost perfectly reproduced: in particular, the net charge on the nitrosyl O atom is increased from –0.30 calculated for the isolated molecule to –0.70 for the polarized molecule.

Hence, this simple model demonstrates firstly that isolated molecules, unperturbed by intermolecular forces, have molecular electronic structures best represented by the classical form *A* (see §3.1), albeit with some modest delocalization involving the exocyclic amino groups; and secondly, that the presence of an external polarizing agency, as typically found in crystalline solids, can readily perturb the molecular–electronic structure towards that described by the canonical form *B*, itself the best single representation of the experimentally observed structures in (1)–(5). Form *B* in turn can lead to the development of very short intermolecular O–H···O hydrogen bonds; it seems likely that the formation of the strong hydrogen bonds and the electronic polarization are acting synergistically.

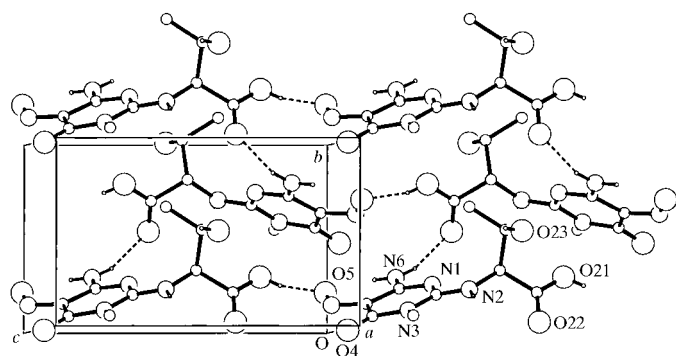


Figure 12

Part of the crystal structure of (5), showing the formation by translation of *C*(11) chains linking the (001) sheets. Atoms are depicted as in Fig. 5.

3.4. Supramolecular structures

3.4.1. Compound (3). The molecules of (3) are linked into a continuous three-dimensional framework by means of O–H···O and N–H···O hydrogen bonds (Table 5). The very short intermolecular hydrogen bond between the carboxylic acid function and the nitrosyl group generates chains by translation, while the intermolecular N–H···O hydrogen bonds generate spirals around screw axes. The two intermolecular N–H···O hydrogen bonds each independently generate a spiral, parallel to the [100] and [010] directions, respectively, while the combination of the two generates a third spiral chain, parallel to [001]. Atom O21 in the carboxylic function at (x, y, z) acts as a donor to nitrosyl O5 at $(x, -1 + y, z)$, thus producing a *C*(11) chain running parallel to the [010] direction (Fig. 5). N2 at (x, y, z) acts as a donor to the amide oxygen O4 at $(-x, -\frac{1}{2} + y, \frac{1}{2} - z)$, while N2 at $(-x, -\frac{1}{2} + y, \frac{1}{2} - z)$ in turn acts as a donor to O4 at $(x, -1 + y, z)$, thus generating a *C*(6) spiral chain around the 2_1 axis along $(0, y, 0.25)$ (Fig. 5). The *C*(11) chain and the *C*(6) spiral together generate $R_3^3(17)$ rings (Fig. 5).

Similarly, N6 at (x, y, z) acts as a donor to carboxylic oxygen O22 at $(\frac{1}{2} + x, \frac{1}{2} - y, -z)$, with N6 at $(\frac{1}{2} + x, \frac{1}{2} - y, -z)$ acting as a donor to O22 at $(1 + x, y, z)$, thus generating a *C*(9) spiral around the 2_1 axis along $(x, 0.25, 0)$ (Fig. 6). The two spirals parallel to [100] and [010] utilize all the molecules within the unit cell and thus necessarily generate a third spiral running parallel to [001], in which the two types of intermolecular N–H···O hydrogen bond generate a $C_2^2(11)$ motif (Fig. 7). The combined effect of the [100], [010] and [001] spirals is to link all the molecules into a single three-dimensional framework.

3.4.2. Compound (4). In the selected asymmetric unit in (4) the water molecule is linked to the amide oxygen O4 by means of an O–H···O hydrogen bond (Fig. 2 and Table 4). These bimolecular aggregates are then linked into spiral chains running parallel to [001] by means of further, paired O–H···O hydrogen bonds and these [001] chains are linked into a two-dimensional sheet by N–H···O hydrogen bonds.

The carboxylic oxygen O21 at (x, y, z) acts as a donor to O5 at $(\frac{3}{2} - x, -y, -\frac{1}{2} + z)$, resulting in the formation of a *C*(11) spiral running parallel to the [001] direction around the 2_1 axis along $(0.75, 0, z)$. At the same time the water molecule at (x, y, z) acts as a donor to carboxylic oxygen O22 at $(\frac{3}{2} - x, -y, \frac{1}{2} + z)$, thus generating a complementary $C_2^2(11)$ spiral around the same screw axis: within the resulting [001] spiral are embedded $R_3^2(12)$ rings (Fig. 8). Parallel [001] chains separated by translation along the [010] direction are linked into a two-dimensional sheet: N6 at (x, y, z) acts as a donor to the amide oxygen O4 at $(x, 1 + y, z)$, thus generating a *C*(6) chain (Fig. 8). The combination of the translational [010] chains and the [001] spirals generates a sheet parallel to (100) and built from $R_3^2(6)$, $R_3^3(12)$ and $R_4^4(26)$ rings: although one of the N–H···O hydrogen bonds is fairly weak (Table 5), the cooperative nature of the hydrogen bonds in generating the (100) is evident (Fig. 8).

The formation of this (100) net utilizes only half of the unit-cell contents and hence two such nets run through each unit

Table 5
Hydrogen-bond geometry (Å, °).

	$D \cdots A$	$H \cdots A$	$D-H \cdots A$	Motif	Direction
(3)					
N6—H6B \cdots O5	2.609 (3)	2.00	127	$S(6)$	
N2—H2 \cdots O4 ⁱ	3.146 (3)	2.35	154	$C(6)$ spiral	[010]
N6—H6A \cdots O22 ⁱⁱ	2.915 (3)	2.06	172	$C(9)$ spiral	[100]
O21—H21 \cdots O5 ⁱⁱⁱ	2.483 (3)	1.65	163	$C(11)$ translation	[010]
(4)					
N6—H6B \cdots O5	2.614 (5)	1.99	129	$S(6)$	
N6—H6A \cdots O4 ^{iv}	3.017 (5)	2.21	155	$C(6)$ translation	[010]
N6—H6B \cdots O1 ^{iv}	2.903 (5)	2.39	118	D	
O11—H11 \cdots O22 ^v	2.693 (5)	1.84	146	$C_2^2(11)$ spiral	[001]
O1—H12 \cdots O4	2.845 (5)	1.98	155	D	
O21—H21 \cdots O5 ^{vi}	2.504 (4)	1.71	161	$C(11)$ spiral	[001]
(5)					
N6—H6B \cdots O5	2.579 (2)	1.95	129	$S(6)$	
N2—H2 \cdots O23 ^{vii}	2.940 (3)	2.08	154	$C(5)$ spiral	[010]
N6—H6A \cdots O22 ^{viii}	2.843 (3)	2.02	161	$C(9)$ spiral	[010]
O21—H21 \cdots O5 ^{ix}	2.440 (2)	1.65	161	$C(11)$ translation	[001]
O23—H23 \cdots O22 ^x	2.716 (2)	1.94	157	$C(6)$ spiral	[010]

Symmetry codes: (i) $-x, -\frac{1}{2} + y, \frac{1}{2} - z$; (ii) $\frac{1}{2} + x, \frac{1}{2} - y, -z$; (iii) $x, -1 + y, z$; (iv) $x, 1 + y, z$; (v) $\frac{3}{2} - x, -y, \frac{1}{2} + z$; (vi) $\frac{3}{2} - x, -y, -\frac{1}{2} + z$; (vii) $2 - x, -\frac{1}{2} + y, 1 - z$; (viii) $1 - x, \frac{1}{2} + y, 1 - z$; (ix) $x, y, -1 + z$; (x) $2 - x, \frac{1}{2} + y, 1 - z$.

cell. The intermolecular hydrogen-bonding components of the two nets lie in the domains $0.15 < x < 0.35$ and $0.65 < x < 0.85$, respectively, so that neighbouring nets are not interwoven.

3.4.3. Compound (5). The molecules of (5) are linked into a continuous three-dimensional framework by two types of N—H \cdots O hydrogen bond and two types of O—H \cdots O hydrogen bond: both hydroxyl groups and both amino groups acts as donors in intermolecular hydrogen bonds and all of the O atoms, except for the amidic O4 and the carboxylic O21 (Fig. 3), act as acceptors of intermolecular hydrogen bonds.

The molecules are linked into spiral chains running parallel to the [010] direction by both N—H \cdots O and O—H \cdots O hydrogen bonds. Atom N2 at (x, y, z) acts as a donor to hydroxyl O23 at $(2 - x, -\frac{1}{2} + y, 1 - z)$, thus generating a $C(5)$ spiral around the 2_1 axis along $(1, y, \frac{1}{2})$. Similarly, O23 at (x, y, z) acts as a donor to carbonyl O22 at $(2 - x, \frac{1}{2} + y, 1 - z)$, producing a $C(6)$ spiral around the same 2_1 axis. Embedded within this [010] chain are $R_2^2(7)$ rings (Fig. 9). The molecules are also linked into [010] spirals around the 2_1 axis along $(\frac{1}{2}, y, \frac{1}{2})$: N6 at (x, y, z) acts as a donor to the carbonyl O22 at $(1 - x, \frac{1}{2} + y, 1 - z)$, thus generating a $C(9)$ spiral (Fig. 10). Carbonyl oxygen O22 thus acts as a double acceptor of hydrogen bonds, while hydroxyl O23 acts as both donor and acceptor (Table 4).

The interaction of these two types of [010] spiral generates a two-dimensional sheet parallel to (001) (Fig. 11) and these sheets are connected into a three-dimensional framework by means of the very short O—H \cdots O hydrogen bonds having the nitrosyl oxygen as an acceptor (Table 4). Carboxylic O21 at (x, y, z) acts as a donor to nitrosyl O5 at $(x, y, -1 + z)$, producing by translation a $C(11)$ chain running parallel to [001], and these chains link each (001) sheet to its two immediate neighbours with concomitant formation of $R_4^4(30)$ rings (Fig. 12).

3.4.4. General comments on the supramolecular structures. There are a number of common features in the supramolecular structures of (3)–(5) which are also shared by those of (1) (Low *et al.*, 1997) and (2) (Low *et al.*, 1999), despite the fact that (1) and (4) crystallize as a dihydrate and as a monohydrate, respectively. In each structure there is a very short intermolecular hydrogen bond between a carboxylic acid group in one molecule, acting as a hydrogen-bond donor, and the nitrosyl O of a neighbouring molecule, acting as an acceptor. This always generates a $C(11)$ motif: in (2) and (3) this motif is generated by translation, in each of (4) and (5) it forms a spiral generated by a 2_1 screw axis, and in (1) it forms a zigzag chain generated by a glide plane.

Secondly, in all compounds except (4), all the N—H bonds are involved in hydrogen bonding: there is always an intramolecular $S(6)$ motif, but the other two N—H bonds [one only in (4)] are donors in intermolecular N—H \cdots O hydrogen bonds. In both of (2) and (3) the N—H \cdots O hydrogen bonds generate $C(6)$ and $C(9)$ spirals with O4 and O22, respectively, as acceptors: a similar $C(6)$ motif, but generated by translation is present in (4), while the usual $C(9)$ spiral is present in (5). Thirdly, the amidic oxygen O4 appears in this series to be a rather weak acceptor of hydrogen bonds; it plays no part in the supramolecular structures of either (1) or (5) and in the remaining compounds it forms only rather long, and hence weak, hydrogen bonds, with N \cdots O distances always in excess of 3.00 Å and an O \cdots O distance above 2.80 Å in (4) (Table 5). By contrast, the other carbonyl oxygen, O22 in the carboxylic acid group, always acts as an acceptor in reasonably short hydrogen bonds and indeed is a double acceptor of such bonds in (5). It is interesting to note the contrast in behaviour of the hydroxylic oxygen O23 between (5), where it acts as both a donor and acceptor of hydrogen bonds, and (4) where it does not participate at all in the hydrogen-bonding scheme (Table 5).

4. Concluding comments

Comparison with related examples drawn from the CSD has confirmed that some of the bond lengths in (1)–(5) are highly unusual: computational modelling using the reference (6) has provided a simple interpretation for the intramolecular geometry which concurrently provides an interpretation of the observed very short intermolecular O—H \cdots O hydrogen bonds. The understanding of the subtle interplay between intra- and intermolecular structure has required the cooperative use of molecular modelling and database analysis.

The nature of the molecular–electronic structures, deduced from both the experimental structural parameters and modelling studies, indicates that the carboxylic acid and the C-nitroso functionalities are likely to be effective ligating sites towards metal ions. The spatial separation of these two func-

ationalities at the opposite vertices of the pyrimidine moiety would prevent their cooperative binding to single metal centres, but opens the possibility of their acting as bridging ligands in the formation of coordination polymers (Moreno *et al.*, 1999), although the formation of extensively hydrogen-bonded salts with metal aqua-ions is also a possibility (Arranz Mascarós *et al.*, 1999, 2000).

References

- Allen, F. H. & Kennard O. (1993). *Chem. Des. Autom. News*, **8**, 31–37.
- Allen, F. H., Kennard, O., Watson, D. G., Brammer, L., Orpen, A. G. & Taylor, R. (1987). *J. Chem. Soc. Perkin Trans. 2*, pp. S1–S19.
- Arranz Mascarós, P., Cobo Domingo, J., Godino Salido, M., Gutiérrez Valero, M. D., López Garzón, R. & Low, J. N. (2000). *Acta Cryst. C56*, e4–e5.
- Arranz Mascarós, P., Godino, M. L., López, R., Cuesta, R., Valenzuela Calahorro, C. & Martín Ramos, D. (1999). *Acta Cryst. C55*, 2049–2051.
- Bauer, S. H. & Andreassen, A. L. (1972). *J. Phys. Chem.* **76**, 3099–3108.
- Bernstein, J., Davis, R. E., Shimon, L. & Chang, N.-L. (1995). *Angew. Chem. Int. Ed. Engl.* **34**, 1555–1573.
- Davis, M. I., Boggs, J. E., Coffey, D. & Hanson, H. P. (1965). *J. Phys. Chem.* **69**, 3727–3730.
- Dewar, M. J. S., Zoebisch, E. G., Healy, E. F. & Stewart, J. J. P. (1985). *J. Am. Chem. Soc.* **107**, 3902–3909.
- Domasevitch, K. V., Gerasimchuk, N. N., Rusanov, E. B. & Gerasimchuk, O. A. (1996). *Zh. Obshch. Khim.* **66**, 652–657.
- Domasevitch, K. V., Mokhir, A. A. & Rusanov, E. B. (1996). *Zh. Obshch. Khim.* **66**, 1501–1505.
- Domasevitch, K. V., Ponomareva, V. V. & Rusanov, E. B. (1997). *J. Chem. Soc. Dalton Trans.* pp. 1177–1180.
- Domasevitch, K. V., Ponomareva, V. V., Rusanov, E. B., Gelbrich, T., Sieler, J. & Skopenko, V. V. (1998). *Inorg. Chim. Acta*, **268**, 93–101.
- Enraf-Nonius (1992). *CAD4 PC Software*. Version 1.1. Enraf-Nonius, Delft, The Netherlands.
- Ferguson, G. (1998). *PREP8*. University of Guelph, Canada.
- Ferguson, G. (1999). *PRPKAPPA*. University of Guelph, Canada.
- Gabe, E. J., Le Page, Y., Charland, J.-P., Lee, F. L. & White, P. S. (1989). *J. Appl. Cryst.* **22**, 384–387.
- Griffin, R. J. & Lowe, P. R. (1992). *J. Chem. Soc. Perkin Trans. 1*, pp. 1811–1819.
- Hamelin, M. (1976). *Acta Cryst.* **B32**, 364–370.
- Korvenranta, J., Näsäkkälä, M., Saarinen, H. & Näsäkkälä, E. (1978). *Acta Chem. Scand. A*, **32**, 533–538.
- Lehn, J.-M., Mascal, M., DeCian, A. & Fischer, J. (1990). *J. Chem. Soc. Chem. Commun.* pp. 479–481.
- Low, J. N., Ferguson, G., López, R., Arranz, P., Cobo, J., Melguizo, M., Nogueras, M. & Sánchez, A. (1997). *Acta Cryst. C53*, 890–892.
- Low, J. N., Godino, M. L., López, R., Pérez, A., Melguizo, M. & Cobo, J. (1999). *Acta Cryst. C55*, 1727–1730.
- Low, J. N., Scrimgeour, S. N., Egglisshaw, C., Howie, R. A., Moreno-Carretero, M. N. & Hueso-Urena, F. (1994). *Acta Cryst. C50*, 1329–1333.
- Maag, H., Locher, R., Daly, J. J. & Kompis, I. (1986). *Helv. Chim. Acta*, **69**, 887–897.
- Moreno, J. M., Arranz Mascarós, P., López Garzón, R., Gutiérrez Valero, M. D., Godino Salido, M. L. & Cobo Domingo, J. (1999). *Polyhedron*, **18**, 1635–1640.
- Nonius (1997). *Kappa-CCD Server Software*. Windows 3.11 Version, Nonius BV, Delft, The Netherlands.
- Otwinowski, Z. & Minor, W. (1997). *Methods Enzymol.* **276**, 307–326.
- Pecorari, P., Rinaldi, M., Costi, M. P. & Antolini, L. (1991). *J. Heterocycl. Chem.* **28**, 891–898.
- Raston, C. L., Sharma, R. P., Skelton, B. W. & White, A. H. (1978). *Aust. J. Chem.* **31**, 745–755.
- Schlemper, E. O., Murmann, R. K. & Hussain, M. S. (1986). *Acta Cryst. C42*, 1739–1743.
- Schwabenlander, F., Kirfel, A. & Mueller, C. E. (1998). *Z. Kristallogr.* **213**, 141–142.
- Sheldrick, G. M. (1997a). *SHELXL97*. University of Göttingen, Germany.
- Sheldrick, G. M. (1997b). *SHELXS97*. University of Göttingen, Germany.
- Shimizu, N., Nishigaki, S., Nakai, Y. & Osaki, K. (1982). *Acta Cryst. B38*, 2309–2311.
- Spek, A. L. (1999). *PLATON*. Version of October 1999. University of Utrecht, The Netherlands.
- Stewart, J. J. P. (1990). *MOPAC 6.0*. Quantum Chemistry Program Exchange, Bloomington, Indiana, USA.
- Talberg, H. J. (1975). *Acta Chem. Scand. A*, **29**, 919–926.
- Talberg, H. J. (1977). *Acta Chem. Scand. A*, **31**, 485–491.
- Wilson, A. J. C. (1976). *Acta Cryst. A32*, 994–996.